INHALED SIMVASTATIN NANOPARTICLES FOR INFLAMMATORY LUNG DISEASE

Alaa S. Tulbah[1, 2], Elvira Pisano[3], Santo Scalia[3], Paul M. Young[1], Daniela Traini[1] and Hui Xin Ong[1*]

[1]Respiratory Technology, Woolcock Institute of Medical Research and Discipline of Pharmacology, Sydney Medical School, Sydney University, NSW, 2037, Australia
[2]Faculty of Pharmacy, Umm Al Qura University, Makkah, Saudi Arabia
[3]Department of Chemical and Pharmaceutical Sciences, University of Ferrara, Italy

*Corresponding author:
Hui Xin Ong
Respiratory Technology, Woolcock Institute of Medical Research and Discipline of Pharmacology, Sydney Medical School, Sydney University, NSW, 2037, Australia
E-mail: ong.hui@sydney.edu.au

ACKNOWLEDGEMENTS

Alaa Tulbah is also grateful to Umm Al-Qura University for their support.

DECLARATION OF INTEREST

The authors declare that there are no conflicts of interest.

1.0 ABSTRACT

Current inhaled treatments are not adequate to treat chronic lung diseases, as most therapies are focused on delaying the onset of irreversible lung damage and slowing disease progression, more than curing the underlying causes of disease. In this study, a promising nanotechnology technology has been developed to deliver a potential anti-inflammatory and muco-inhibitory compound, simvastatin, for treatment of inflammatory lung diseases via inhalation. Simvastatin nanoparticles (SV-NPs) were fabricated using polymer constituents with the aim to improve its stability, in vitro cytotoxicity and efficacy. The SV-NP generated was found to be stable up to 9 months at storage of 4 °C and nebulisation of the SV-NP formulation showed promising aerosolisation properties, with fine particle fraction (FPF) of 45.15 ± 8.15%. The *in vitro* cytotoxicity assay showed that SV-NPs were at least 10X less toxic to lung epithelial cells compared to SV solution. Additionally, transport studies revealed that SV-NPs were able to control the release of SV over time and can penetrate into the airway epithelial cells and subsequently convert into its active SVA metabolite for its pharmacological action. In terms of efficacy, the amount of mucus produced was significantly reduced after SV-NP treatment on an inflamed epithelial cell model. In addition, SV-NPs were effective in suppressing the expression of the pro-inflammatory markers; interleukin (IL)-6, IL-8 and tumour necrosis factor-alpha (TNF- α) after 24 and 48 h following lipopolysaccharide (LPS) stimulation of the cell airway model. This study suggests that nebulisation of SV-NPs could potentially be used for the localised treatment of airway inflammation and hyper-mucus production in patients with chronic pulmonary diseases.

KEYWORDS: Simvastatin; nanoparticles; inhalation; stability; epithelia transport; mucus; inflammation.

2.0 INTRODUCTION

The method by which drugs are delivered can have significant impact on its efficacy and numerous drug delivery systems have been already developed to control the pharmacokinetics, pharmacodynamics, toxicity and efficacy of these kind of formulations. Significant research efforts into drug carrier systems (i.e. polymeric nanoparticles, liposomes and micelles) have been undertaken over the past decade due to its significant advantages in different routes of administration, including pulmonary inhalation, oral and transdermal formulation in reducing drug degradation, prevention of harmful side effects and targeted delivery (1). Aerosol therapy has been preferentially used for the local treatment of a variety diseases such as lung infections, asthma, cystic fibrosis and chronic obstructive pulmonary diseases (COPD), instead of the other different administration routes (2, 3). This is because the lung have a large alveolar surface area that allows for rapid drug absorption, avoidance of first-pass metabolism and reduced risk of systemic side effects (4).

The World Health Organisation (WHO) has predicted that COPD to be the 3rd most common cause of death by 2020. Most of the current treatments are focused on symptom alleviation in order to improve patient's quality of life, by treatments with inhalation of β-agonist for bronchodilation, antibiotics to treat infection and corticosteroids as anti-inflammatory agents (5). A significant proportion of these patients develop 'drug resistant refractory effect' towards these treatments after prolonged administration (6). Furthermore, there is currently no marketed treatment that reduces mucus over production in the respiratory tract, which is a hallmark feature of COPD (7). Therefore, development of a new or alternative treatment option that will improve efficacy in the treatment of chronic respiratory diseases are of paramount importance to overcome the refractory drug effects.

Simvastatin (SV) has conventionally been used as an oral anti-cholesterol drug for the treatment of hyperlipidemia, acting inhibitor of the 3-hydroxy-3-methyl-glutaryl-Coenzyme A (HMG-CoA) reductase enzyme. Besides the cholesterol lowering effect, it has recently been found that SV possesses muco-inhibitory effect, immuno-

modulatory and anti-inflammatory properties unrelated to its anti-cholesterol effect (5, 8, 9). These properties of SV have attracted much attention for treatment of various lungs conditions including asthma and COPD where inflammation, oxidative stress and mucus overproduction are main hallmark features (9-18). Despite this, oral SV (lipophilic prodrug) is easily hydrolysed into its active metabolite simvastatin hydroxy acid (SVA), which will become poorly absorbed in the body as well as into the lung cells. These have been the major drawbacks hampering its clinical application for the treatment of lung diseases, as demonstrated in the conflicting clinical results in regards to its efficacy (13).

Therefore, one possible way to overcome these drawbacks and ensure high concentration of drugs being delivered directly to the target site, is through direct administration of inhaled SV to the lungs, subsequently reducing the risk of systemic side-effects as well as preventing first-pass metabolism (19, 20). Specifically, nebulising therapy has been widely used to convert liquids into aerosols of a size suitable for lung delivery. Other advantages of using nebulization includes delivery of drugs in solution form (21) and ease of use of these apparatuses by the patients, which does not require breath/hand coordination (22).

As SV has low water solubility and is very chemically unstable, nanoparticle technology have been utilised to improve SV stability, pharmacokinetic profiles, bioavailability and reduced toxicity of lung diseases treatment (23).

In this study, poly (Lactic-Co-Glycolic Acid) [PLGA] (a well-studied polymer for drug applications and has been approved by Food and Drug Administration (FDA)) has been used to formulate and deliver SV-NP (24, 25). In addition, pluronic®F-127 (hydrophilic nontoxic copolymer) was used as an excipient in the formulation to improve drugs stability and increase drug solubility (26). In fact, several studies have shown that encapsulation of drug within polymeric layer materials such as PLGA or pluronic are not only able to improve drug's stability (27) but also increase its efficacy (28-31).

This study will focus on the development of a stable polymeric SV nanoparticle formulation for nebulisation as a potential alternative therapeutic approach or adjunct therapy for treatment of inflammatory lung diseases. This novel formulation was

characterised in terms of its physico-chemical properties, *in vitro* aerosol performance and long-term chemical stability. More importantly, the efficacy and toxicity of SV nanoparticles formulation was evaluated for its ability to transport across the airway epithelial cells, activation into the SVA, reduced mucus production and inflammation activity.

Formatted: Highlight

3.0 MATERIALS AND METHODS

3.1 Materials

Simvastatin was used as supplied (Jayco Chemical Industries. Thane, India). Simvastatin hydroxy acid (SVA) was manufactured in house according the following procedure: 41.8 mg of SV were dissolved in 1 mL of absolute ethanol; 1.5 mL of NaOH 1N were added to the SV ethanol solution. The solution was subsequently incubated at 50°C. After 2 h, the pH of the solution was adjusted to 7.2 with HCl and deionised water was then added to the solution up to 10 mL and the final SVA solution was stored at -20°C until use [11].

Pluronic F-127, dimethylsulfoxide (DMSO), and Poly (Lactic-Co-Glycolic) acid (PLGA) 75:25 (average MW = 66,000–107,000) were obtained from Sigma Aldrich, Australia. While, solvents such as ethanol, methanol and acetonitrile were purchased from Thermo-Fisher, Australia. All chemicals were used without further purification. Water was purified by reverse osmosis (MilliQ, Millipore, France). All other solvents used were of analytical grade and were supplied by Bio-lab (Victoria, Australia).

Calu-3 cells were purchased from the American Type Culture Collection (Manassas, USA). All cell culture reagents including Dulbecco's modified Eagle's medium (DMEM), phosphate-buffered saline, trypsin–EDTA solution (2.5 g/ L trypsin, 0.5 g/L EDTA), foetal bovine serum, L-glutamine solution (200 mM) and Hank's balanced salt solution (HBSS) were obtained from Invitrogen (Sydney, Australia). Transwell cell culture inserts (0.33 cm^2 polyester, 0.4 µm pore size) were purchased from Corning Costar (Lowell, MA, USA). Protease inhibitor cocktail and non-essential amino acids solution, CelLytic™ M Cell Lysis were purchased from Sigma-

Aldrich (Sydney, Australia). All other sterile culture plastic wares were purchased from Sarstedt (Adelaide, Australia).

3.2 Preparation of PLGA encapsulated SV Nanoparticles (SV-NPs)

Polymeric SV nanoparticles formulation (SV-NPs) were fabricated using a solvent and anti-solvent precipitation method. Briefly, 5% w/v of SV was first dissolved in dichloromethane (DCM). This SV solution was subsequently added to a chilled Pluronic F-127 (3 mg/mL) aqueous solution dropwise to a concentration of 2% v/v and homogenized (Silver- son L4RT, East Longmeadow, MA, USA) at 6,000 rpm for 2 min on ice. The mixture was then added into a solution consisting of 50 mg/mL of PLGA in DCM solution and homogenised at the same speed for another 2-3 min to encapsulate the nanoparticles with PLGA. Following that, the nanoparticles were collected and washed 3 times with distilled water by centrifugation using the Amicon® Ultra-15 Centrifugal filter unit (10 kDa) at 2750 rpm; 4ºC about 45-60 min. The resultant formulation was stored at -80 ºC for 1 h prior to lyophilisation at -50 ºC for 24 hours (B. Braun, Melsungen, Germany).

3.3 Particle Characterisation of SV-NPs suspension

3.3.1 Particle Size Analysis: Dynamic Light Scattering (DLS) and Transmission Electron Microscopy (TEM)

The particle size and polydispersity index (PDI) of SV-NPs were determined by dynamic light scattering (DLS) (Nano Series ZS Zetasizer, Malvern Instruments, Worcestershire, UK). Approximately 1 mg/mL of SV-NP re-suspended in deionized water and sonicated prior to analysis. Size measurements were carried out in triplicate at 25 ºC. The morphology of SV-NPs was assessed using TEM (JEOL 1400, Tokyo, Japan). Samples of SV- NPs suspension (0.1 mg/mL) was prepared in phosphate buffer solution (PBS) at pH 7.4, then sonicated on an ice bath for 1 min. The diluted suspension (one drop) was added on to a 200-mesh carbon-coated TEM grid and allowed to air-dry. The grids were subjected to 4% of osmium tetroxide used to stain the TEM grids and increased the contrast, dried at ambient temperature and immediately imaged with TEM at 120 kV.

3.3.2 Chemical Stability of SV-NPs

The chemical stability of unencapsulated SV solution and SV-NPs formulation was assessed up to 10 days and 9 month, respectively at 4°C with the drugs protected from light. The chemical stability of the formulation was performed by weighing 1mg of the samples i.e. raw SV or SV-NPs and dissolving it into 1 ml of acetonitrile: water (65:35 v/v). Then, the samples immediately analysed for SV and its metabolite, SVA using the validated high performance liquid chromatography (HPLC) method. The experiment was tested in triplicates.

3.3.3 Encapsulation efficiency of SV-NPs

The encapsulation efficiency of freshly made SV-NPs formulation was determined by ultrafiltration. SV-NPs were added into ultrafiltration tubes (Amicon, Ultra-0.5, Millipore, USA). Then, the tubes were centrifuge for 15 min at 16,000 g. The filtered solution was collected at the bottom of ultrafiltration tubes (containing free SV). The HPLC was used to determine simvastatin content and unfiltered SV-NPs.

The % of encapsulation efficiency was estimated based on the equation below:

$$\text{Encapsulation efficiency } (\%) = \frac{Unfiltered\ SV - filtered\ solution\ (free\ SV)}{Unfiltered\ SV} \times 100$$

3.3.4 Simvastatin (SV) and Simvastatin Acid Analysis (SVA)

Quantification of SV and its metabolite SVA was performed using HPLC. A Shimadzu HPLC system consisting of a LC20AT pump, the SIL20AHT auto-sampler and an SPD-20A UV-VIS detector (Shimadzu, Sydney, NSW, Australia) was used. The mobile phase mixture comprised of acetonitrile: water (65:35 v/v) and 0.025 M sodium dihydrogen phosphate with pH adjusted to 4.5 with phosphoric acid. The mobile phase was then filtered under vacuum. Analysis of SV was achieved using a reverse phase C-18 column (Phenomenex ODS hypersclone) 250 X 4.6 mm, 5-µm particle size. The HPLC system was set to the following conditions: UV detector wavelength 238 nm, 100 µL injection volume and flow rate 1.5 mL/min. Retention time for SV was 9.1 and for SVA was 5.5 minutes, respectively. Linearity was

obtained between 0.01 and 50 µg/mL (R^2=0.99) for both SV and SVA.

3.3.5 Droplet Size Measurement Using Laser Diffraction

Aerosol droplet produced after nebulisation of the SV-NPs formulation using a PARI LC Sprint® nebuliser powered by the Pari Turbo Boy S compressor (Starnberg, Germany) was evaluated where assessed for aerodynamic size using Laser diffraction technique. This was achieved using the Malvern Spraytec (Malvern Instrument Ltd., Worcestershire, UK) with an open bench configuration and minimal distance between the nebuliser's mouthpiece and laser measurement to minimise droplet evaporation, as previously described (23). Air extraction by a vacuum operating at 15 L/min airflow calibrated using a flowmeter (TSI 3063, TSI instruments Ltd., Buckinghamshire, UK) was used to prevent aerosol re-entry into measuring zone. The reservoir of the nebuliser was filled with 2 mL of the SV-NPs (5mg/mL) formulation prior to nebulisation. The measurements were made at room temperature and 30% relative humidity (RH). After setting up the airflow through the flow cell, aerosol size measurements were initiated 5 s prior to nebulisation and measurements were captured for 60s. The samples were analysed in triplicates. For data analysis, detectors 1-6 were excluded to account for beam steering and an algorithm to correct multiple scatter within the Malvern software was activated. All measurements were at 70>% of light transmission and vignetting for ensuring the absence of multiple scattering. Geometric standard deviation (GSD) and median droplet size were determined by averaging all data points excluding the first and last 10 s of nebulisations.

Formatted: Highlight

3.3.6 Cascade Impaction analysis

Further characterisation of the nebulised aerosols for aerosol performance and correlation with laser diffractometry was performed using the next generation impactor (NGI, Copley Scientific, Nottingham, UK). The aerosol performance was performed at days 7 and 9-months' time point to ensure stability of the formulation. Prior to the measurements, the NGI flow rate was set at 15 L min^{-1} using a flow meter

and controlled by a GAST rotary vein pump and solenoid valve timer set for 60s (Westech Scientific Instruments, Bedfordshire, UK). This set-up was in accordance to the British Pharmacopeia (Apparatus E) standard, which mimicked the tidal breathing of an adult. Then, 2 mL of the SV-NPs formulation (5 mg/mL in PBS) were added into PARI LC Sprint® nebuliser and the nebuliser was fitted into the mouthpiece adapter, which was subsequently connected to the NGI using a United States Pharmacopeia (USP) throat. Each sample was tested in triplicate.

After nebulisation, the device, mouthpiece adapter, USP throat and NGI cups were oven dried at 70°C to evaporate the aqueous phase before cooling to ambient temperature for subsequent mass recovery assay. All of the components were rinsed individually using acetonitrile: water (65:35 v/v) and analysed using HPLC as described above.

Formatted: Highlight

Aerosol performance was assessed upon the classification of fine inhalable particles as those with an aerodynamic diameter <5µm. The emitted dose (ED) was defined as the total mass deposited in the mouthpiece adapter, USP throat and NGI cups. The fine particle fraction (FPF), mass median aerodynamic diameter (MMAD) and the geometric standard deviation (GSD) was calculated from the regression of log-linear plots of stage-size verses cumulative stage deposition.

3.3.7 Thermal Properties Analysis

A differential scanning calorimeter (DSC1 -Mettler-Toledo Ltd, Switzerland) was used to determine the thermal properties of the SV-NPs and was compared to the un-processed SV, Pluronic and PLGA alone. Approximately, 10mg of pre-weighed SV-NPs was sealed in a 40 µL aluminium pan and samples were heated under a N_2 atmosphere at a rate of 10 °C/min between 25°C to 300°C. Temperatures of each exothermic and endothermic peak and their onset were determined using STARe V11.0Å~ software (Mettler-Toledo). Data were normalised for initial mass.

Formatted: Highlight

Formatted: Highlight

Formatted: Highlight

3.3.8 Dynamic Vapour Sorption

Dynamic vapour sorption (DVS- Intrinsic 1, Mettler-Toledo Ltd, Switzerland) was used to analyse the water uptake of both un-processed and SV-NPs at different RH. Both samples (11mg) were dried at 0% RH before exposure to two sorption cycles of 0 to 90 % RH at 10% increment for two cycles. The change in mass-to-time ratio (dm/dt) of 0.0005%/min was used to determine equilibrium od moisture sorption and the profiles of the samples were determined by an automated water sorption analyser.

Formatted: Highlight

3.3.9 Drug Release Profile

Prior to the drug release experiments, dialysis membranes (MW cut-off 6000–8000, Cellu.Sep, Texas, USA) were soaked in 100 mL of phosphate buffered saline (PBS) for 20 min to ensure thorough wetting of the membrane. The pore size of the dialysis bag was chosen to allow free diffusion of SV solution and simultaneously prevent the exit of SV-NPs into the sink phase. This study was carried out in PBS at pH 7.4 over 4h period. SV-NPs suspension and free SV solution (5 mL) were enclosed in the dialysis bag, which was immersed in 100 mL of PBS solution to ensure sink conditions. The solutions were maintained at 37 °C in a water bath under constant agitation using a magnetic stirrer (300 rpm). Samples of 500 uL were withdrawn ever 30 min from the sink medium and were replaced with equal volumes of fresh PBS. All experiments were performed in triplicate. SV and SVA content was analysed using HPLC.

3.4 In Vitro Bio-Characterisation

Bronchial Calu-3 epithelial cell line was cultured between passages 37–47 in pre-warmed DMEM medium—F12 supplemented with 1% (v/v) L-glutamine solution, 1% (v/v) non-essential amino acid solution and 10% (v/v) foetal bovine serum. Cells were incubated until confluency was reached at 37°C in 5% CO_2 and 95% humidity. Medium was exchanged every 2– 3 days and weekly, the cells were passaged according to ATCC recommended guidelines (32-34).

3.4.1 SV-NPs and un-processed SV epithelia cell cytotoxicity assay

The cytotoxicity of SV-NPs formulation and SV solution (2 mM) was evaluated in vitro using Calu-3 cells as previously described (33)(17). Briefly, the cells were seeded into sterile 96-well plates at a density of 5×10^5 cell/cm^2. Then, the plate was incubated overnight at 37 °C in 5% CO_2 humidified atmosphere to allow for attachment. Subsequently, the cells were treated with different concentrations (from 0.01 nM to 1000 µM) of SV. SV solution was prepared by dissolving SV into 100% ethanol to prepare the stock solution and then diluted in DMEM medium to a final ethanol concentration of <2%, ensuring negligible toxicity to the cells. The SV-NPs were suspended in DMEM medium alone to the same concentration as SV solution. The cells were treated for 3 days and incubated at 95% RH and 37°C in 5% CO^2 and was followed by cytotoxicity assay using CellTiter 96® Aqueous One Solution Cell proliferation A reagent (Promega, Australia) for another 3 h. The colour intensity was measured at 490 nm of absorbance using a fluorescence microplate reader (SpectraMax M2; Molecular devices, USA). Cell viability was determined as the percentage of viable cells relative to the untreated control, as previously described (34, 35). The drug concentration that produced a decrease of 50% in cell viability were defined as IC50 values and compared to the untreated control. IC50 values were calculated by plotting (%) cell viability against the concentrations (ng/mL) on a logarithmic scale. Data were fitted to the Hill equation using the General Fit function of GraphPad Prism 6 software (GraphPad Software, Inc. CA 92037 USA).

Formatted: Highlight

3.4.2 Transepithelial Drug Transport Studies

Transport studies were performed on air-interface Calu-3 cells (5×10^5 cell/cm^2 density) seeded on to Transwell polyester inserts (Corning Costar, USA), where the medium was aspirated from the apical chamber 24 hours post-seeding as described previously (32, 34). To allow for cell differentiation, the transport experiments were performed between days 11 and 14 of culture. SV-NPs formulation was nebulised onto the air interface epithelial model using a modified glass twin stage impinger (TSI; Copley Scientific, UK) at a flow rate of 15 L/min for 5s. This allowed particles ≤ 6.4 cm aerodynamic diameter to deposit onto the epithelial cells to simulate *in vivo* aerosol deposition in the lungs as previously described (34, 36). Samples were

consequently taken from the basolateral chamber of the Transwell every 1 h for up to four hours and replaced with fresh transport buffer (Hanks Buffered Salt Solution, Sigma, Australia). After that, drugs remaining on and inside the Calu-3 cells were analysed to quantitative the SV and SVA recover concentration to obtain the total initially deposited dose. The integrity of the cell monolayer was also assessed after SV-NPs exposure onto the Calu-3 cells. This was performed using the transepithelial electrical resistance (TEER) measurements with a voltohmmeter (EVOM, World Precision Instruments, USA) as previously described (32, 36) and subsequently compared with untreated cells.

3.4.3 Mucus Inhibition Study

Similarly, to assess the ability of the SV-NPs formulation to inhibit mucus overproduction, the formulation was nebulised on to Calu-3 cells at day 11 using the modified TSI. Prior to drug deposition, the Calu-3 cells were stimulated with 1 ng/mL of LPS for 24 h to stimulate inflammation. Mucus analysis was performed on day 14 where mucus glycoproteins were stained with alcian blue as previously described (32, 33) to allow the visualisation of mucus on the surface of Calu-3 cells after SV-NPs deposition and compared with untreated cells (control). Initially, PBS was used to wash the cells and then 4% paraformaldehyde (PFA) was added for 20 minutes to fix the cells. Then, PFA was removed, cells rinsed twice with PBS and alcian blue (100 µL) added for 15 min for mucus staining. The stain was then removed by washing PBS and inserts left to dry. Finally, cells were mounted onto glass slides with mounting medium and sealed. All samples were stored in the fridge prior to analysis. The Olympus BX60 microscope (Olympus, Tokyo, Japan) equipped with an Olympus DP71 camera (Wetzlar, Germany) to capture the images. Apple Automator (v 2.0.4 Apple Inc., Cupertino, California, USA) was used to convert the images into TIFF files for analysis using ImageJ (v1.42q, NIH) with Colour Profile (Dimiter Prodanov; Leiden University Medical Center, Leiden, Netherlands). The ratio of red, green, blue (RGB ratio) was calculated by dividing the mean RGB by the sum of the RGB values for each image (RGBR + RGBG + RGBB). The mean RGB was used to quantify mucus production, in both the control and the SV-NPs treated cells.

3.4.4 Measurements of Inflammatory Responses

The *in vitro* concentrations of inflammatory cytokine, including interleukin-6 (IL-6), interleukin- 8 (IL-8) and tumour necrosis factor- α (TNF-α), after treatment with SV-NPs and vitamin E (positive control) was analysed using human ELISA Kit II IL-6, IL-8 and TNF-α (BD OptEIATM, catalogue number 265KI, 2645KI and 2637KI, BD Biosciences, San Diego, California, USA) according to the manufacturer's instructions. Similar to the mucus study, the epithelial cells were stimulated with 1 ng/mL of LPS 24 h prior to deposition of any treatment. The cells were treated with nebulised SV-NPs, and 2.6 mg/mL of vitamin E (positive controls) and compared to untreated cells. The epithelial cells were incubated at 37°C, 5% CO_2 and medium samples were collected at for 24 and 48h h to allow for the production of pro-inflammatory cytokines. The quantities of secreted IL-6, IL-8 and TNF-α in the test samples were determined using a standard curve measured with purified recombinant human IL-6, IL-8 and TNF-α provided with the kit. The limits of for IL-6, IL-8 and TNF-α detection were 4.6–300 pg/mL, 3.1–200 pg/mL and 7.8–500 pg/mL, respectively.

Formatted: Highlight

3.5 Statistical Analysis

All results are expressed as mean ± standard deviation (S.D.) of at least three separate determinants. To determine significance between groups and control, unpaired two-tailed t-tests and one-way ANOVA were performed (quoted at the level of $p<0.05$).).

4.0 RESULTS AND DISCUSSION

To overcome SV issues of instability and poor aqueous solubility, SV was repurposed as a nebulised polymeric SV-NPs for the treatment of inflammatory respiratory diseases. In this study, SV-NPs coated with PLGA and pluronic-F127 as stabilisers were prepared. The SV-NPs formulation was assessed in terms of their physio-chemical properties, chemiocal stability, aerosol performance and its efficacy in terms of mucus inhibition, release profiles and anti-inflammatory activity using *in vitro* methodologies. The *in vitro* data supports the concept that inhaled polymeric SV-NPs formulations could become an important new approach for the treatment of inflammation and mucus overproduction in patients with chronic lung diseases.

Formatted: Highlight

4.1 SV-NPs Formulation Characterisation

4.1.1 Characterisation of SV-NPs

The size distribution and morphology of SV-NPs formulation after freeze drying was determined using DLS and TEM, respectively. The mean diameter of SV-NPs particles was found to be 213.8± 6.69 nm, with a polydispersity index of < 0.1, indicating a narrow size distribution. The transmission electron micrograph (Figure 1) shows that the freeze-dried SV-NPs suspended in PBS appear to be spherical in shape, with their sizes estimated to be around 175 nm. This finding is in good agreement with the particle size distribution data but somewhat larger than the observed size. This may be due to the indirect size measurement methods of DLS, which is based on the calculation of mean size of the sample population rated than the physical diameter (23). Furthermore, the encapsulation efficiency prepared using this method was high, at approximately 99.5%.

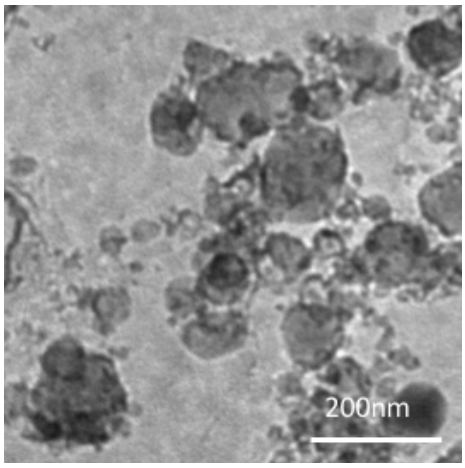

Figure 1: Transmission electron micrograph of polymeric SV-NPs formulation.

4.1.2 Stability of SV-NPs

The stability of SV (prodrug) within the NPs is of utmost importance in the formulation of inhalation therapy to ensure absorption into the airway epithelium and hence efficacy of treatment. SV is very susceptible to hydrolysis in the presence of water causing the opening of the lactone ring to form the SVA metabolite. This is evident in Figure 2A, which demonstrate that approximately 38% of SV in solution, has degraded into SVA within the first day and complete degradation is observed within 7 days. This is a significant problem associated with formulating SV for inhaled nebuliser solution. Although SVA is the active form of SV, hydrolysis prior to absorption will render SVA incapable of being transported into the pulmonary cells limiting its pharmacological actions. It is therefore essential to ensure the maintenance of SV stability within the NPs.

Formatted: Highlight

The chemical stability of SV-NPs formulation up to 9 month of the storage at 4°C is shown in Figure 2. The SV-NPs formulation showed no significant chemical degradation to the active metabolite SVA up to 9-month, with all values quantified within pharmacopoeia specification of ± 25 % (British Pharmacopoeia 2010) of the nominal dose. Results showed that the powder had no significant degradation, with an average dose of 39.6 ± 8.99 µg of SV in 1mg of powder, during 9-month period. The

Formatted: Highlight

presence of SVA was also chemically analysed and found not to change over the 9-month period (average value 1.74 ± 1.50 µg that is equivalent to 4.84 ± 4.15 % of the nominal dose).

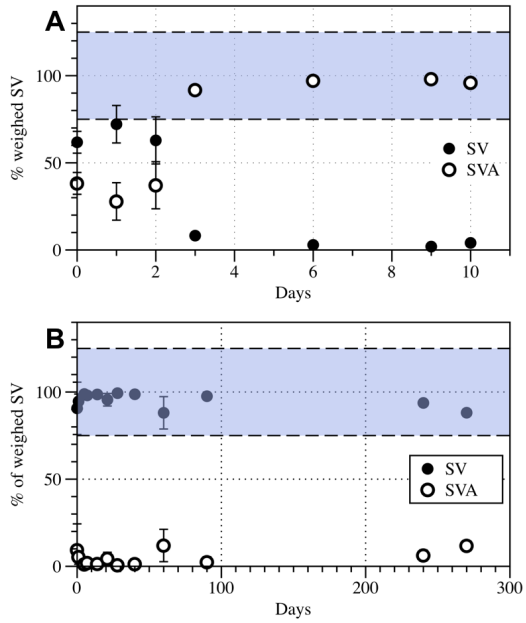

Figure 2: The stability of (A) SV in solution up to 10 days of storage at 4°C and (B) SV-NPs up to 9 months of storage at 4°C, (n=3± SD). Dotted lines indicate the ± 25 % BP pharmacopoeia limit.

4.1.3 In vitro aerodynamic evaluation of nebulised SV-NPs formulation

The characteristics of the aerosols generated from the nebuliser as determined using laser diffraction and cascade impaction are shown in Figure 3 and Table 1, respectively. Laser diffraction technique is an established alternative to cascade impaction and can be used for nebulised droplets size characterisation using unit density spheres approximation. Analysis of the percentile undersize values showed that nebulised SV-NPs aerosols to have values of $D_{0.1=}$0.31 ± 0.01 µm, $D_{0.5=}$ 3.61 ± 0.13 µm and $D_{0.9=}$ 8.98 ±0.13µm, respectively, with a span of 2.40 ± 0.07, indicating that the aerosol possessed a suitable size for drug delivery to the lung. Previous

studies have found high levels of correlation between geometric diameter of droplets from laser diffraction and aerodynamic droplets diameter from cascade impaction (37, 38). However, laser diffraction suffers from beam stearing, multiple scatter and vignetting in addition to varying data interpretation that could lead to varying data interpretation. Therefore, *in vitro* aerosolisation studies were performed using the NGI to validate the results that was obtained from laser diffraction.

Formatted: Highlight

The deposition of the nebulised SV-NPs formulation on each stage of the NGI after nebulisation are shown in Figure 3B. Data are represented as the percentage of the total drug deposited in the mouthpiece, induction port and each of the NGI cup over the emitted dose from the device. Aerosol performance parameters such as FPF, MMAD and GSD were calculated from the log regression plot of these data and presented in Table 1. In addition, aerosol performance study was performed on the 1st, 6th and 9th month to ensure stability of the formulation. The aerosol performance parameters were found to be not statistically different between the 3 times points studied (p>0.05). These results confirm that the SV-NPs formulation was stable up to 9 months. Furthermore, the median droplet sizes from both the laser diffraction and cascade impaction were compared and was found to be not significantly different and suitable for deep lung delivery. It is also important to note that the SV-NPs formulation remained stable with more than 86.2 ± 4.3% of SV unchanged after the nebulisation of the suspension.

	MMAD (µm ± SD)	GSD	FPF (% ± SD)
1m	4.73 ± 0.28	2.43 ± 0.33	46.07± 2.96
6m	4.11 ± 1.53	2.86 ± 0.47	45.5 ± 8.73
9m	4.21 ± 0.78	2.83 ± 0.53	42.59 ± 7.14

Table 1: The nebulised SV-NP aerosol characteristics at 1, 6 and 9 months using NGI cascade impaction (n =3, ± SD)

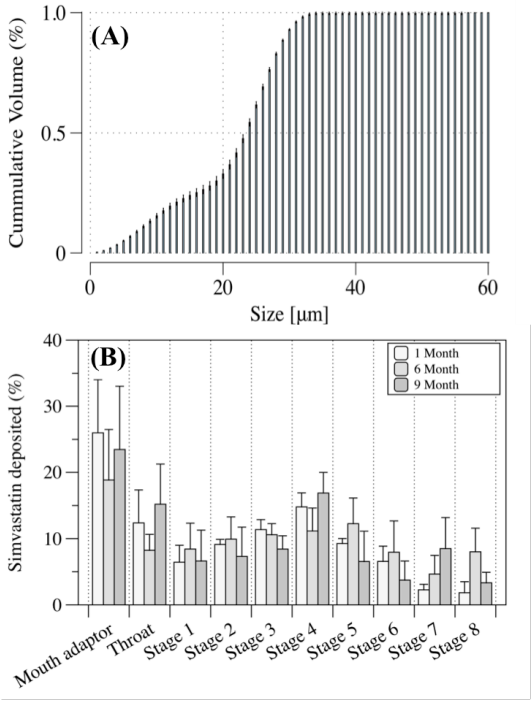

Figure 3: (A) In-line laser diffraction particle size measurement and, (B) NGI stage deposition data of nebulised SV-NPs formulations (n=3, ± SD).

4.1.4 Thermal Properties Analysis

The thermal behaviors of the SV-NPs together with the respective raw materials (i.e. SV, pluronic and PLGA) were characterised using DSC and TGA. The DSC thermographs of the SV-NPs and raw materials are shown in Figure 4. An endothermic peak that correlated to the melting point of the un-processed SV was found to be at 141.17 °C. This is in good correlation with a previous study (39) and is characteristic of a crystalline behavior. However, the endothermic peak of SV within the SV-NPs was not clear but was consistent with the endothermic peaks of Pluronic F-127 and the PLGA components. Analysis of the other raw components of SV-NPs,

PLGA and Pluronic F-127, showed an endothermic reaction at 53°C and 59°C corresponding to their glass transition temperature (40) and melting point (41), respectively. These DSC results could be attributed to the low 5% of SV in the sample and lead to interactions (encapsulation) between Pluronic F-127 and the drug.

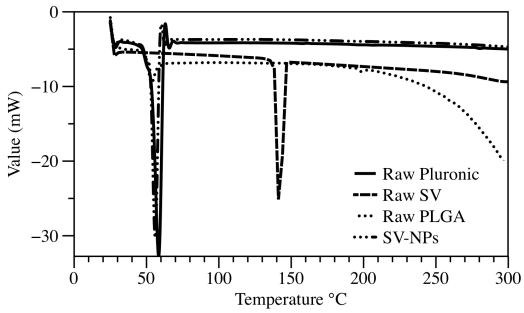

Figure 4: Differential scanning calorimetry of un-processed SV material and SV-NPs suspension.

4.1.5 Dynamic Vapour Sorption

The effect of humidity on moisture sorption was analysed by DVS to understand the relative stability of SV-NPs formulation solid state. Figure 5 demonstrates the moisture sorption profiles (1st and 2nd sorption and desorption cycles) of SV-NPs. Between 0 and 90% RH, the formulations displayed crystalline behaviour with no detectable amorphous material presence. This is noted from the presence of reversibility moisture hysteresis profiles that was reproduced during the second exposure cycle (42). The SV-NPs also displayed a double sigmoidal type (S) curve during both moisture sorption and desorption. A maximum mass change of 1.9% was recorded at 90% RH. This is significantly higher compared to the raw and dry powder formulations of SV in previous study that showed a maximum mass change of 0.18%. This observation could be attributed to multilayer water sorption onto the larger surfaces that are available of the SV-NPs sample as well as the other components of the formulation affecting the surface chemistry of the formulation (43).

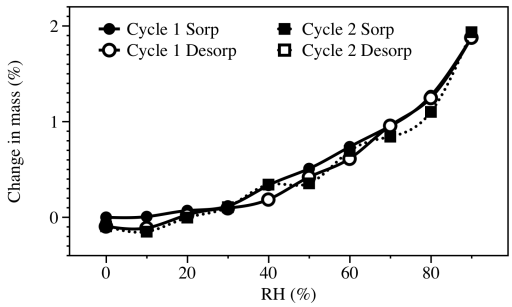

Figure 5: Dynamic vapour sorption isotherms of SV-NPs, two cycles from 0 to 90 RH %.

4.1.6 Drug Release Profile and chemical Stability of SV-NPs

The release profiles of SV-NPs and SV solution formulation across a dialysis membrane was studied in PBS at pH 7.4 and 37 °C is shown in Figure 6. The SV solution formulation demonstrated rapid SV diffusion from the dialysis bag with >41.53% of the drug released over the 4 h experiment, suggesting no retardation of drug diffusion across the dialysis membrane. While, the release profiles from the SV-NPs formulations suggested sustained release over the 4 h period with approximately half of the SV (21.2%) being released from the polymeric NPs. This could be beneficial to reduce dosing frequency of these new therapy and improve patient compliance.

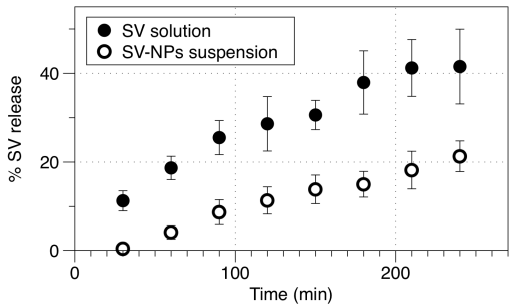

Figure 6: *In vitro* drug release profiles of SV-NPs and solution formulation across a dialysis membrane from the (n = 3, mean ± SD).

4.2 In vitro bio-characterisation

4.2.1 *Cytotoxicity of SV-NPs*

. The *in vitro* cytotoxicity on bronchial Calu-3 epithelial cells of the SV-NPs formulation was evaluated and was subsequently compared to SV solution to understand the range of concentrations suitable for pulmonary drug delivery (Figure 7). The Calu-3 cells were treated with different ranges of SV concentration in solution or within the nanoparticles, from 0.01 nM to 1000 µM up to 72 h. It was found that SV-NPs was at least 15 times less toxic than SV solution with IC50 values of 178.3 ± 1.27 µM and 10.79 µM ± 1.44 µM, respectively. These data suggest that SV-NPs is significantly less toxic and safer compared to un-encapsulated SV, supporting its potential delivery to the lungs as a treatment for chronic lung diseases. Furthermore, the improved cytotoxicity of the SV-NPs can be attributed to the polymeric nanoparticle shell that protects the cells from coming in direct contact with the SV drug.

Formatted: Highlight

Formatted: Highlight

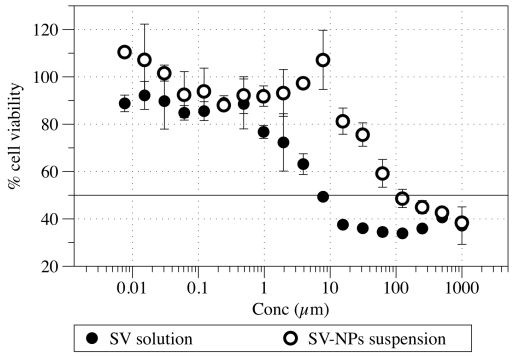

Figure 7: Concentration-dependent cytotoxicity of SV solution and SV-NPs formulation on Calu-3 cells. Data are expressed as mean ± SD of three independent replicates.

4.2.2 *Transport Studies*

The transport of the nebulised SV-NPs formulation shown in Figure 8A and B, was assessed using the modified TSI coupled with the air interface Calu-3 cell model. The

deposition of respirable SV-NPs aerosols onto the mucosa surfaces of lung epithelial cells (44) enables the evaluation of SV release from the polymeric nano-encapsulation, ability of released SV to penetrate into airway epithelial cells and finally provide an estimate conversion to the SVA metabolite. Drug amounts were expressed as the mean cumulative percentage (± SD) of the total drug recovered throughout the experiments. The total drug (SV+SVA) deposited onto the Calu-3 epithelial cell layer was found to be 1.23 ± 0.07 µg. Figure 8A shows the transport of SV and SVA as a function of time with approximately 12.16 ± 5.77 % of SV and 7.07 ± 1.33 % of SVA that were able to transport across the epithelial cells over the 4 h transport experiment. As for the remainder of the drug, a total of 59.98 ± 5.32 % remained on the surface of the cells, while 13.45 ± 3.70% were found inside the cells. The proportion of intracellullar SV and SVA was found to be 12.14 ± 2.86 % and 1.31 ± 0.93, respectively. Although, this amount of SVA conversion was significantly lower compared to previous inhaled SV pMDI (18) and DPI (17) formulations development, nevertheless it demonstrates the capacity of the epithelium to activate SV to SVA that is essential for their immuno-modulatory effects (33). These observations of lower transport and activation rates of SV, coupled with the high amounts of drugs remaining on the epithelium, further demonstrates the controlled release properties of the polymeric nanoparticle encapsulation. Hence, upon deposition of liquid aerosols containing the SV-NPs onto the epithelium, the SV is slowly released into the surrounding epithelia lining fluid. This limiting factor subsequently controls the diffusion of SV into the epithelial cells and hence conversion to the active SVA counterparts by the carboxylesterases and cytochrome P450 enzymes.

After the transport studies, the integrity of the Calu-3 monolayer was evaluated using TEER measurements (Figure 8C). There was no significant change in resistance compared with the control (SV-NPs: 486.97 ± 32.21 Ωcm^2 and control: 538.49 ± 74.03 Ωcm^2, respectively). Hence, it can be concluded that the high local concentrations of SV-NPs after aerosol deposition had no harmful effects on the epithelial cell integrity under the conditions and time scale studied, which was in agreement with the cytotoxicity findings.

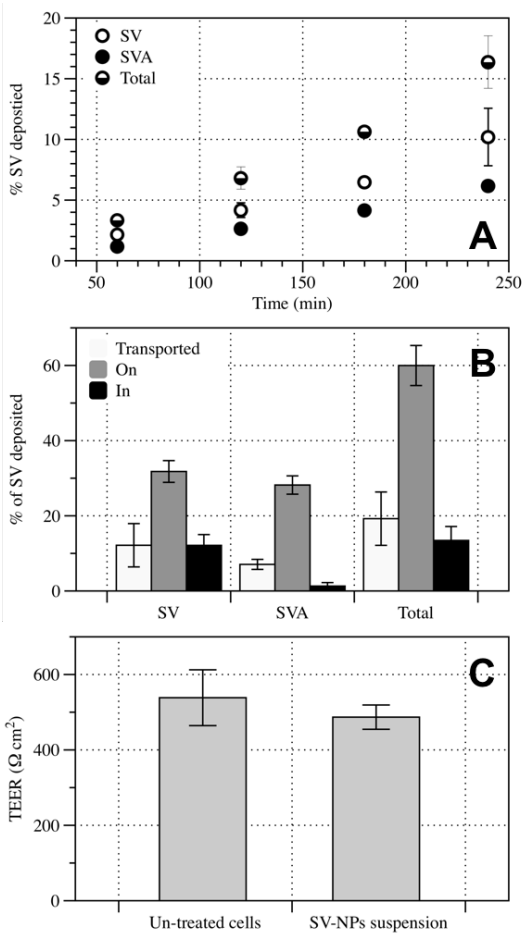

Figure 8: (A) Transport of SV, SVA and total drug amount (SV+SVA) as a function of time, (B) Cumulative amounts of SV, SVA and Total (SV+SVA) recovered in the cells, remaining on the cells and transported across the Calu-3 cells and (C) Transepithelial electrical resistance (TEER), 4 hours after the deposition of SV-NPs, (n=3 ± SD).

4.2.3 *Mucus studies*

Mucus over-production in the airways is considered one of the more challenging symptoms to treat, as current therapies are only able to help clear mucus from the airways but not to reduce its production. A previous study in rat airways has

suggested that SV's muco-inhibitory effect is mediated by the inhibition of the extracellular signal-regulation kinase (ERK) activation pathway within the goblet cells to attenuate mucin synthesis induced with the acrolein (13, 45). In this study, the ability of inhaled SV-NPs formulation to inhibit mucus production was assessed on LPS induced epithelial cells. The formulation was aerosolised onto the inflamed cell model using the modified TSI set-up, similar to the transport study at day 11 of culture. Three days after SV-NPs deposition, the mucus was examined and compared with untreated control by calculating the intensity of the blue stained mucus using the RGB ratio values of the microscopic images taken for each condition. The SV-NPs formulations showed significant inhibition of mucus production compared to the untreated controls at day 14 ($p<0.05$) with reduction in the RGB ratio in Figure 9A and B. In addition, TEER measurements after the study showed no significant difference in monolayer integrity after the pro-longed SV-NPs exposure (Figure 9C), demonstrating that SV-NPs are safe and not detrimental to the epithelium. The slow release of SV in combination with enhanced cytotoxicity of the polymeric nano-encapsulation of the drugs could explains the differing results observed with previous inhaled SV formulations that demonstrated a loss of monolayer integrity (16, 18).

Formatted: Highlight

Formatted: Highlight

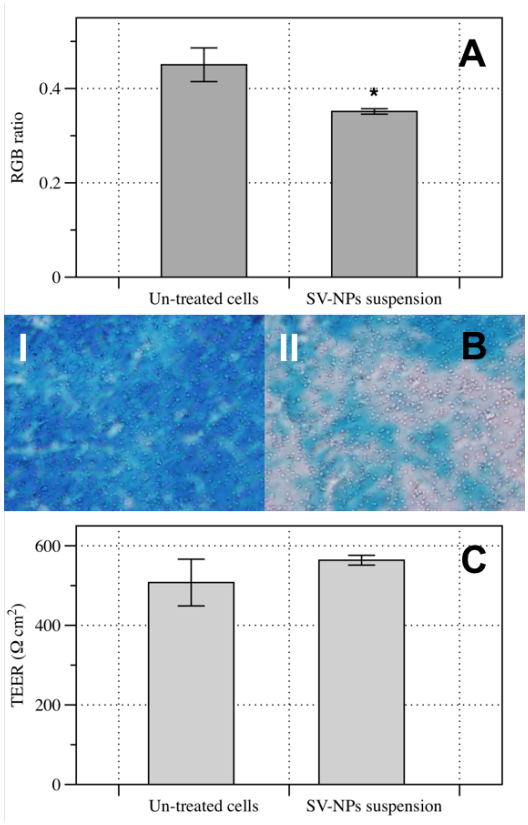

Figure 9: (A) RGB ratio of alcian blue intensity at day 14 of untreated control and after the deposition of SV-NPs onto inflamed Calu-3 cells, (n = 3 ± S.D.), (B) Microscopic images of alcian blue stained mucus on the epithelium at day 14 of (I) untreated cells and (II) SV-NPs treated cells and (C) The effect of SV-NPs on TEER following the deposition in the mucus study after 3 days exposure.

4.2.4 *Inflammatory Effects of SV-NPs Formulation on IL-6, 8 and TNF-α production*

After demonstrating the ability of nebulised SV-NPs to reduce mucus production in addition to gradually releasing SV, penetrate and activate SV to SVA in the epithelium, it is essential to investigate the efficacy of the SV-NP formulation as anti-inflammatory agent. Another hallmark feature of chronic lung diseases is the over-

expressions of pro-inflammatory cytokines such as IL-6, IL-8 and TNF- α. Progressive inflammation in these diseases often lead to the activation and migration of neutrophils to the lungs, causing further irritation and irreversible damage to the lung tissues (46-48). Although many studies have found that SV was able to reduce airway inflammation in murine models of asthma, clinical data have showed otherwise, which may be due to it systemic mode of delivery (49, 50).

In this study, the potential of SV-NPs to reduce pro-inflammatory chemokines production (IL-6, IL-8 and TNF-α) was investigated following stimulation of Calu-3 epithelial cells with LPS 24-h prior to drug deposition. LPS is a known bacteria endotoxin (51, 52) used to simulate an inflammatory condition and chemokine concentration was quantified 24 and 48 h post treatment. Analysis of the data demonstrates that nebulised SV-NPs, as well as Vit E control, were effective in downregulating the expressions of IL-6, IL-8 and TNF-α in inflamed epithelium at both 24 and 48 h (Figure 10) compared with untreated cells. However, no statistical difference was found between the Vit E and SV-NP formulation, with the different chemokines. Used for this investigation. Interestingly, there was a significant reduction in IL-6, IL-8 and TNF-α production after 48 h of SV-NPs treatment (Figure 10B), compared to both untreated cells and Vit E treatment. These results could be correlated to added stability of polymeric SV-NPs and sustain release of SV over time, leading to improved anti-inflammatory actions. Inhibition of the NF-κB activation pathway by SV is the proposed immune-modulatory mechanism that lead to reductions in inflammatory mediator production as well the reduced mucus production. However, this will require future investigation. Similar findings by Sakoda *et al.* that demonstrates a reduction in IL-6 and IL-8 expressions due to the inhibition of NF-κB activity through Rac1 GTPase inhibition in oral epithelial cells following SV treatment for periodontitis (53).

Formatted: Highlight

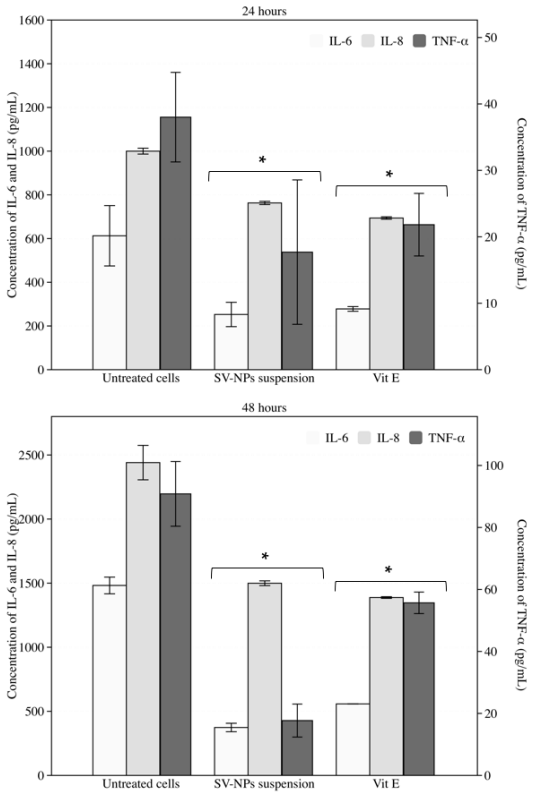

Figure 10: Immuno-modulatory effects of nebulised SV-NPs compared to controls (vitamin E and LPS) on IL-6, IL-8 and TNF-α levels produced by Calu-3 epithelial cells after (A) 24 h and (B) 48 h. Data represents mean ± S.D., (n=3). *p<0.05, statistically different to untreated cells**.**

5.0 CONCLUSIONS

In conclusion, SV-NPs formulation was successfully formulated for inhalation using polymeric nanoparticle technologies and characterised *in vitro*. This study has demonstrated that the formulation was stable up to 9 months and suitable for nebulisation in to the deep lungs. Furthermore, it was shown to possess controlled release properties that could be beneficial for sustained anti-inflammatory properties, reducing absorption and allowing higher SV concentrations to remain in the airways for therapeutic efficacy and reducing mucus production. Hence, SV-NP formulation has the potential to be used as an adjunct or alternative treatment for chronic pulmonary diseases with uncontrolled inflammation and mucus overproduction.

Formatted: Highlight

6.0 REFERENCES

1. Azarmi S, Roa WH, Lobenberg R. Targeted delivery of nanoparticles for the treatment of lung diseases. Adv Drug Deliv Rev. 2008;60(8):863-75.
2. Dhanani J, Fraser JF, Chan H-K, Rello J, Cohen J, Roberts JA. Fundamentals of aerosol therapy in critical care. Critical Care. 2016;20(1):269.
3. Patton JS, Platz RM. (D) Routes of delivery: Case studies:(2) Pulmonary delivery of peptides and proteins for systemic action. Advanced Drug Delivery Reviews. 1992;8(2-3):179-96.
4. Johnson KA. Preparation of peptide and protein powders for inhalation. Advanced drug delivery reviews. 1997;26(1):3-15.
5. Yang Y, Tsifansky MD, Shin S, Lin Q, Yeo Y. Mannitol-guided delivery of Ciprofloxacin in artificial cystic fibrosis mucus model. Biotechnol Bioeng. 2011;108(6):1441-9.
6. Barnes PJ, Adcock IM. Glucocorticoid resistance in inflammatory diseases. The Lancet. 2009;373(9678):1905-17.
7. Turner J, Jones CE. Regulation of mucin expression in respiratory diseases. Portland Press Limited; 2009.
8. Tobert JA. Lovastatin and beyond: the history of the HMG-CoA reductase inhibitors. Nat Rev Drug Discov. 2003;2(7):517-26.
9. Endo A, Tsujita Y, Kuroda M, Tanzawa K. Inhibition of cholesterol synthesis in vitro and in vivo by ML-236A and ML-236B, competitive inhibitors of 3-hydroxy-3-methylglutaryl-coenzyme A reductase. Eur J Biochem. 1977;77(1):31-6.
10. Vaughan CJ, Murphy MB, Buckley BM. Statins do more than just lower cholesterol. Lancet. 1996;348(9034):1079-82.
11. McAuley DF, O'Kane CM, Craig TR, Shyamsundar M, Herwald H, Dib K. Simvastatin decreases the level of heparin-binding protein in patients with acute lung injury. BMC Pulm Med. 2013;13:47.
12. Grommes J, Vijayan S, Drechsler M, Hartwig H, Morgelin M, Dembinski R, et al. Simvastatin reduces endotoxin-induced acute lung injury by decreasing neutrophil recruitment and radical formation. PLoS One. 2012;7(6):e38917.
13. Tulbah AS, Ong HX, Colombo P, Young PM, Traini D. Could simvastatin be considered as a potential therapy for chronic lung diseases? A debate on the pros and cons. Expert opinion on drug delivery. 2016;13(10):1407-20.
14. Rezaie-Majd A, Maca T, Bucek RA, Valent P, Muller MR, Husslein P, et al. Simvastatin reduces expression of cytokines interleukin-6, interleukin-8, and monocyte chemoattractant protein-1 in circulating monocytes from hypercholesterolemic patients. Arterioscler Thromb Vasc Biol. 2002;22(7):1194-9.
15. Blamoun A, Batty G, DeBari V, Rashid A, Sheikh M, Khan M. Statins may reduce episodes of exacerbation and the requirement for intubation in patients with COPD: evidence from a retrospective cohort study. Int J Clin Pract. 2008;62(9):1373-8.
16. Tulbah AS, Ong HX, Colombo P, Young PM, Traini D. Novel simvastatin inhalation formulation and characterisation. AAPS PharmSciTech. 2014;15(4):956-62.

17. Tulbah AS, Ong HX, Morgan L, Colombo P, Young PM, Traini D. Dry powder formulation of simvastatin. Expert opinion on drug delivery. 2015;12(6):857-68.
18. Tulbah AS, Ong HX, Lee W-H, Colombo P, Young PM, Traini D. Biological effects of simvastatin formulated as pMDI on pulmonary epithelial cells. Pharmaceutical research. 2016;33(1):92-101.
19. Yuan C, Zhou L, Cheng J, Zhang J, Teng Y, Huang M, et al. Statins as potential therapeutic drug for asthma? Respiratory research. 2012;13(1):108.
20. Labiris N, Dolovich M. Pulmonary drug delivery. Part I: physiological factors affecting therapeutic effectiveness of aerosolized medications. British journal of clinical pharmacology. 2003;56(6):588-99.
21. FAARC DRHPR. Nebulizers: principles and performance. Respiratory care. 2000;45(6):609.
22. Alhaddad B, Smith F, Robertson T, Watman G, Taylor K. Patients' practices and experiences of using nebuliser therapy in the management of COPD at home. BMJ open respiratory research. 2015;2(1):e000076.
23. Ong HX, Traini D, Cipolla D, Gonda I, Bebawy M, Agus H, et al. Liposomal nanoparticles control the uptake of ciprofloxacin across respiratory epithelia. Pharmaceutical research. 2012;29(12):3335-46.
24. Mehanna MM, Mohyeldin SM, Elgindy NA. Respirable nanocarriers as a promising strategy for antitubercular drug delivery. Journal of Controlled Release. 2014;187:183-97.
25. Lee WH, Bebawy M, Loo CY, Luk F, Mason RS, Rohanizadeh R. Fabrication of Curcumin Micellar Nanoparticles with Enhanced Anti-Cancer Activity. J Biomed Nanotechnol. 2015;11(6):1093-105.
26. DeLong RK, Risor A, Kanomata M, Laymon A, Jones B, Zimmerman SD, et al. Characterization of biomolecular nanoconjugates by high-throughput delivery and spectroscopic difference. Nanomedicine. 2012;7(12):1851-62.
27. Bae KH, Ha YJ, Kim C, Lee K-R, Park TG. Pluronic/chitosan shell cross-linked nanocapsules encapsulating magnetic nanoparticles. Journal of Biomaterials Science, Polymer Edition. 2008;19(12):1571-83.
28. Anand P, Nair HB, Sung B, Kunnumakkara AB, Yadav VR, Tekmal RR, et al. RETRACTED: Design of curcumin-loaded PLGA nanoparticles formulation with enhanced cellular uptake, and increased bioactivity in vitro and superior bioavailability in vivo. Biochemical pharmacology. 2010;79(3):330-8.
29. Sou K, Inenaga S, Takeoka S, Tsuchida E. Loading of curcumin into macrophages using lipid-based nanoparticles. International journal of pharmaceutics. 2008;352(1):287-93.
30. Rashidi H, Ellis MJ, Cartmell SH, Chaudhuri JB. Simvastatin release from poly (lactide-co-glycolide) membrane scaffolds. Polymers. 2010;2(4):709-18.
31. Assaf K, Duek EAdR, Oliveira NM. Efficacy of a combination of simvastatin and poly (DL-lactic-co-glycolic acid) in stimulating the regeneration of bone defects. Materials Research. 2013;16(1):215-20.
32. Haghi M, Young PM, Traini D, Jaiswal R, Gong J, Bebawy M. Time- and passage-dependent characteristics of a Calu-3 respiratory epithelial cell model. Drug Dev Ind Pharm. 2010;36(10):1207-14.
33. Marin L, Traini D, Bebawy M, Colombo P, Buttini F, Haghi M, et al. Multiple dosing of simvastatin inhibits airway mucus production of epithelial cells:

implications in the treatment of chronic obstructive airway pathologies. Eur J Pharm Biopharm. 2013;84(3):566-72.
34. Ong HX, Traini D, Bebawy M, Young PM. Epithelial profiling of antibiotic controlled release respiratory formulations. Pharm Res. 2011;28(9):2327-38.
35. Ong HX, Traini D, Ballerin G, Morgan L, Buddle L, Scalia S, et al. Combined Inhaled Salbutamol and Mannitol Therapy for Mucus Hyper-secretion in Pulmonary Diseases. AAPS J. 2014:1-12.
36. Ong HX, Traini D, Salama R, Anderson SD, Daviskas E, Young PM. The effects of mannitol on the transport of ciprofloxacin across respiratory epithelia. Mol Pharm. 2013;10(8):2915-24.
37. Ziegler J, Wachtel H. Comparison of cascade impaction and laser diffraction for particle size distribution measurements. Journal of aerosol medicine. 2005;18(3):311-24.
38. Clark AR. The use of laser diffraction for the evaluation of the aerosol clouds generated by medical nebulizers. International Journal of Pharmaceutics. 1995;115(1):69-78.
39. Murtaza G. Solubility Enhancement of Simvastatin: A Review. Acta Pol Pharm. 2012;69(4):581-90.
40. Lee LY, Wang CH, Smith KA. Micro-porous Paclitaxel-Loaded PLGA Foams--a New Implant Material for Controlled Release of Chemotherapeutic Agents. 2007.
41. Dai J, Kim JC. Photo and thermal properties of cinnamoyl Pluronic F-127. Polymer International. 2014;63(3):501-6.
42. Young PM, Price R, Tobyn MJ, Buttrum M, Dey F. Effect of humidity on aerosolization of micronized drugs. Drug Dev Ind Pharm. 2003;29(9):959-66.
43. Giles CH, MacEwan T, Nakhwa S, Smith D. 786. Studies in adsorption. Part XI. A system of classification of solution adsorption isotherms, and its use in diagnosis of adsorption mechanisms and in measurement of specific surface areas of solids. J Chem Soc. 1960:3973-93.
44. Ong HX, Traini D, Young PM. Pharmaceutical applications of the Calu-3 lung epithelia cell line. Expert Opin Drug Deliv. 2013;10(9):1287-302.
45. Chen YJ, Chen P, Wang HX, Wang T, Chen L, Wang X, et al. Simvastatin attenuates acrolein-induced mucin production in rats: involvement of the Ras/extracellular signal-regulated kinase pathway. Int Immunopharmacol. 2010;10(6):685-93.
46. Hothersall E, McSharry C, Thomson NC. Potential therapeutic role for statins in respiratory disease. Thorax. 2006;61(8):729-34.
47. Burrows B, Knudson RJ, Cline MG, Lebowitz MD. Quantitative Relationships between Cigarette Smoking and Ventilatory Function 1, 2. American Review of Respiratory Disease. 1977;115(2):195-205.
48. Burnett D, Hill S, Chamba A, Stockley R. Neutrophils from subjects with chronic obstructive lung disease show enhanced chemotaxis and extracellular proteolysis. The Lancet. 1987;330(8567):1043-6.
49. Kim DY, Ryu SY, Lim JE, Lee YS, Ro JY. Anti-inflammatory mechanism of simvastatin in mouse allergic asthma model. European journal of pharmacology. 2007;557(1):76-86.
50. Vaughan CJ, Murphy MB, Buckley BM. Statins do more than just lower cholesterol. The Lancet. 1996;348(9034):1079.

51. Reiter E, Jiang Q, Christen S. Anti-inflammatory properties of α-and γ-tocopherol. Molecular aspects of medicine. 2007;28(5):668-91.
52. Scardino PL, Scott WW. The use of tocopherols in the treatment of Peyronie's disease. Annals of the New York Academy of Sciences. 1949;52(3):390-6.
53. Sakoda K, Yamamoto M, Negishi Y, Liao J, Node K, Izumi Y. Simvastatin decreases IL-6 and IL-8 production in epithelial cells. Journal of dental research. 2006;85(6):520-3.